A Theoretical Analysis of High-nuclearity Metal Carbonyl Clusters *

D. Michael P. Mingos and Lin Zhenyang
Inorganic Chemistry Laboratory, University of Oxford, South Parks Road, Oxford OX1 3QR

Stone's tensor surface Harmonic methodology has been applied to high-nuclearity transition-metal carbonyl cluster compounds with 13—44 metal atoms. In these close-packed metal clusters the metal atoms lie on concentric spheres and the orbital interactions can be simplified significantly if the orbitals are assigned pseudo-spherical symmetry labels. Two limiting bonding situations have been identified and represented in terms of general electron-counting rules. If the radial bonding effects predominate the clusters are characterized by $12n_s + \Delta_i$ valence electrons, where n_s is the number of surface atoms and Δ_i is the characteristic electron count of the interstitial moiety. If radial and tangential bonding effects are important then the total number of valence electrons is $12n_s + 2(s_s + s_i - 1)$, where s_s and s_i are the number of skeletal bonding molecular orbitals associated with surface (s_s) and interstitial (s_i) moieties.

In recent years a very large number of high-nuclearity cluster compounds have been synthesized and structurally characterized.[1—4] A comprehensive review has recently been given by Vargas and Nicholls.[3] In a preliminary communication Mingos[5a] rationalized the bonding patterns in these compounds with 13—44 metal atoms (see Tables 1—3) and found that these clusters are generally characterized by $12n_s + \Delta_i$ valence electrons, where n_s is the number of surface atoms and Δ_i is characteristic of the interstitial group of atoms. For instance, if the interstitial group of atoms is an octahedron, $\Delta_i = 86$, a tetrahedron, $\Delta_i = 60$, and a triangle, $\Delta_i = 48$, *etc.* In this paper, we give a more detailed theoretical analysis of this electron-counting rule using Stone's methodology.[6] This model, which is based on a particle on a sphere free-electron model, is relevant because the observed structures of high-nuclearity clusters (Tables 1—3) can be described in terms of multi-concentric spheres.[7]

The simplest type of high-nuclearity cluster is one where the central metal polyhedron is capped by one or more metal atoms. The theoretical aspects of these clusters have been discussed in some detail elsewhere.[8] The capping principle[9] states that capping a face of a polyhedron leads to no change in the number of skeletal bonding orbitals. Therefore, capping with a transition-metal atom leads only to an increase in cluster valence electron count of 12. Consequently, the general formula for the electron count in high-nuclearity capped clusters can be expressed as $12n_c + \Delta$, where n_c is the number of capping atoms and Δ is the electron count characteristic of the central cluster. A more complicated situation arises when the capping atoms are sufficiently numerous for metal–metal bonds to be formed between them. The bonding in this type of cluster is discussed in this paper.

Bonding Analysis

(1) *The Bonding in High-nuclearity Clusters with One Interstitial Atom.*—Some examples of deltahedral and four-connected clusters with transition-metal and main-group interstitial atoms are summarized in Table 1. Deltahedral clusters have a total of $n_s + 1$ bonding skeletal molecular orbitals[10a,b] and $6n_s$ orbitals which are either non-bonding or involved in metal–ligand bonding. Therefore such clusters are characterized by $12n_s + 2(n_s + 1)$ valence electrons, *i.e.* $14n_s + 2$.[10b] In terms of Stone's notation the metal–ligand bonding occurs primarily through $n_sL^{\pi}_{pd}$, $n_sL^{\sigma}_{sp}$, and $n_s\overline{L^{\pi}_{dp}}$ out-pointing hybrid orbitals and the $n_sL^{\delta}_{d}$, $n_s\overline{L^{\delta}_{d}}$, and $n_sL^{\sigma}_{d}$ are essentially non-bonding. For ML_3 fragments the latter correspond to the 't_{2g}'-like orbitals of an octahedral fragment.[10c] From Table 1, it is apparent that the total number of valence electrons in such clusters does not depend on whether the interstitial atom is a transition-metal or a main-group atom. For example, although the interstitial atom is Pt in $[Rh_{12}Pt(CO)_{24}]^{4-}$,[11] the cluster has the same number of valence electrons ($170 = 12n_s + 26$, *i.e.* 13 skeletal bonding orbitals) as $[Rh_{13}H_5(CO)_{24}]^{12}$ and $[Rh_{12}Sb(CO)_{27}]^{3-}$.[13] Similarly the two octahedral clusters, $[Ru_6C(CO)_{17}]^{14}$ and $[Rh_6(CO)_{16}]$,[15] have the same electron count of 86 although the former has an interstitial carbon atom.

It has been shown[16] that the anti-cuboctahedron and the cuboctahedron have the same number and pattern of skeletal bonding orbitals. Therefore the results of extended-Hückel molecular-orbital calculations on the higher-symmetry structure have been used to develop the principal theoretical arguments. Specifically, calculations on $Rh_{12}H_{36}$ (ML_3 fragment) and $Rh_{13}H_{36}$ (with one central Rh) as shown in (**1**) have been completed.

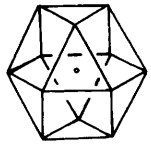

(1)

The Rh_{13} cluster was chosen as a model because the interstitial atom is a transition metal with *s*, *p*, and *d* valence orbitals. Figure 1 shows the important interactions between the interstitial atom and the outer-sphere cluster, Rh_{12}. The non-bonding 't_{2g}' orbitals and the M–L bonding molecular orbitals of the outer-sphere cluster have been omitted from the figure for reasons of clarity. There are a total of $6n_s$ orbitals of this type. The skeletal molecular orbitals for Rh_{12} lie in a narrow energy range and comprise F^{π}, D^{π}, $P^{\pi/\sigma}$, S^{σ}, and F^{π}_{3c}. There are a total of 13 skeletal bonding orbitals. This is a general characteristic of four-connected clusters and this aspect has been discussed in some detail elsewhere.[8] When the central atom is inserted into the Rh_{12} cluster the three *p* orbitals of the central atom stabilize the $P^{\sigma/\pi}$ orbitals slightly. The *s* and *d* orbitals interact strongly with the S^{σ} and D^{π} orbitals of the outer sphere, and give rise to the in-phase combinations $S^{\sigma} + s$ and $D^{\pi} + d$ bonding

* *Non-S.I. unit employed:* eV ≈ 1.60 × 10^{-19} J.

Table 1. Examples of high-nuclearity clusters with one interstitial atom based on the $12(n_s + n_c) + 2n_s + 2$ rule[a]

Compound	n_i	n_s	n_c	Electron count Obs.	Calc.	
$[Rh_{13}H_5(CO)_{24}]$	1	12	0	170	170	$12(n_s + n_c) + 2n_s + 2$
$[Rh_{12}Pt(CO)_{24}]^{4-}$ [b]	1(Pt)	12	0	170	170	
$[Rh_{15}(CO)_{30}]^{3-}$	1	14	0	198	198	
$[Ru_6C(CO)_{17}]$	1(C)	6	0	86	86	
$[Rh_{10}S(CO)_{22}]$	1(S)	10	0	142	142	
$[Rh_{12}Sb(CO)_{27}]$	1(Sb)	12	0	170	170	
$[Os_{10}C(CO)_{24}]^{2-}$	1(C)	6	4	134	134	

n_i = Number of interstitial atoms, n_s = number of surface atoms which are connected directly to the interstitial atoms, and n_c = number of capping atoms.

[a] Ref. 5a. [b] Ref. 11.

Table 2. Examples of high-nuclearity cluster compounds based on the $12n_s + \Delta_i$ electron-counting rule[a]

Compound	n_i	n_s	n_c	Electron count Obs.	Calc.	
$[Au_9(PPh_3)_8]^+$	1	8	0	114	114	$12n_s + 18$
$[Au_{11}I_3(PPh_3)_7]$	1	11	0	138	138	
$[Au_{13}Cl_2(PR_3)_{10}]^{3+}$	1	12	0	162	162	
$[Pt_{15}H_x(CO)_8(PBu_3)_6]$ [b]	1	12	2	$178 + x$	186	$12(n_s + n_c) + 10 + x$ [c]
$[Pt_{19}(CO)_{22}]^{4-}$	2	17	0	238	238	$12(n_s + n_c) + 34$
$[Rh_{22}H_{5-q-m}(CO)_{35}]^{q-}$	2	16	4	$273 + m$	274	
$[Au_{13}Ag_{12}Cl_6(PPh_3)_{12}]^{m+}$	3	22	0	$317 - m$	314	$12n_s + 50$
$[Ni_{38}Pt_6H_{6-n}(CO)_{48}]^{n-}$	6(Pt)	32	6	542	542	$12(n_s + n_c) + 86$
$[Pt_{38}H_m(CO)_{44}]^{2-}$	6(Pt)	32	0	$470 + m$	470	
$[Ni_{34}C_4(H)(CO)_{38}]^{5-}$ [d]	4(Ni) + 4(C)		30	438	438	$12(n_s + n_c) + 78$
$[Ni_{35}C_4(CO)_{39}]^{6-}$ [d]	4(Ni) + 4(C)		31	450	450	
$[Ni_{38}C_6(H)(CO)_{42}]^{5-}$ [e]	8(Ni) + 6(C)		30	494	492	$12(n_s + n_c) + 132$

[a] Ref. 5a. [b] J. A. K. Howard, J. L. Spencer, and D. G. Turner, *J. Chem. Soc., Dalton Trans.*, 1987, 259. [c] Predicted value $x = 8$. [d] Ref. 22. [e] Ref. 21.

Table 3. Examples of high-nuclearity clusters deviating from the electron-counting rules

Compound	n_i	n_s	n_c	Electron count obs.	Comments
$[Pd_{23}(CO)_{22}(PEt_3)_{10}]$ [a]	1	18	4	$294 = 12 \times (16 + 6) + 30$	Occupation of 6 $L_{pd}^{\pi/\sigma}$ in Figure 2
$[Pd_{23}(CO)_{20}(PEt_3)_8]$ [b]	1	14	8	$286 = 12 \times (14 + 18) + 22$	Occupation of 2 $L_{pd}^{\pi/\sigma}$ in Figure 2
$[Pt_{24}(CO)_{30}]$ [c]	1	23	0	$276 = 12 \times 23 + 24$	Occupation of 3 $L_{pd}^{\pi/\sigma}$ in Figure 2
$[Pt_{26}(CO)_{32}]^{2-}$ [c]	3	23	0	$326 = 12 \times 23 + 50$	$> 12n_s + 48$
$[Pd_{38}(CO)_{28}(PEt_3)_{12}]$ [b]	4	22	12	$460 = 12 \times (22 + 12) + 52$	$< 12(n_s + n_c) + 60$

[a] E. G. Mednikov, N. K. Eremendo, Yu. L. Slovokhotov, and Yu. T. Struchkov, *J. Organomet. Chem.*, 1986, **301**, 35. [b] Ref. 18. [c] Ref. 5a.

orbitals, and the out-of-phase combinations $S^\sigma - s$ and $D^\pi - d$ which are antibonding. The F^π orbitals are essentialy unaffected by the introduction of the central atom. Consequently, the interaction between *s*, *p*, and *d* orbitals of the interstitial atom and the skeletal bonding orbitals of the outer sphere leads to no change in the total number of the skeletal bonding orbitals. It is apparent that in the cluster with a main-group interstitial atom the D^π orbitals of the outer sphere are still in the bonding region and fully occupied. Therefore, the clusters with one main-group interstitial atom have the same electron count as the clusters with a transition-metal atom at the centre if both clusters have the same structure. A more detailed analysis of such clusters has been presented elsewhere.[17]

Figure 2 gives a generalized interaction scheme for high-nuclearity clusters with a single interstitial atom. If the metal atoms are evently distributed on the surface of the sphere then there are always a set of nine S^σ, $P^{\sigma/\pi}$, and D^π skeletal molecular orbitals capable of interacting with the *nd*, $(n + 1)s$, and $(n + 1)p$ valence orbitals of the interstitial atom. In addition there are $(n_s - 8)$ $L_{pd}^{\pi/\sigma}$ $(L > 2)$ tangential molecular orbitals with a significant proportion of *p*-orbital character. As the number of metal atoms increases the energy difference between the $L_{pd}^{\pi/\sigma}$ and $\overline{L_{pd}^{\pi}}$ orbitals decreases and the energy gap between the $L_{pd}^{\pi/\sigma}$ and $\overline{L_{pd}^{\pi}}$ orbitals becomes smaller.[5b] For a close-packed arrangement of metal atoms the interstitial atom is surrounded by 12 to 14 metal atoms on a spherical surface and the additional atoms behave as capping atoms and lie on a second concentric spherical surface. It follows therefore from the capping principle[9] that for a close-packed arrangement there is a limiting number of between four and six $L_{pd}^{\pi/\sigma}$ $(L > 2)$ skeletal molecular orbitals. Furthermore, when there are a large number of atoms on the first and second spherical surfaces the energy differences between alternative cubic close packed (c.c.p.), hexagonal close packed (h.c.p.), and body-centred cubic (b.c.c.)

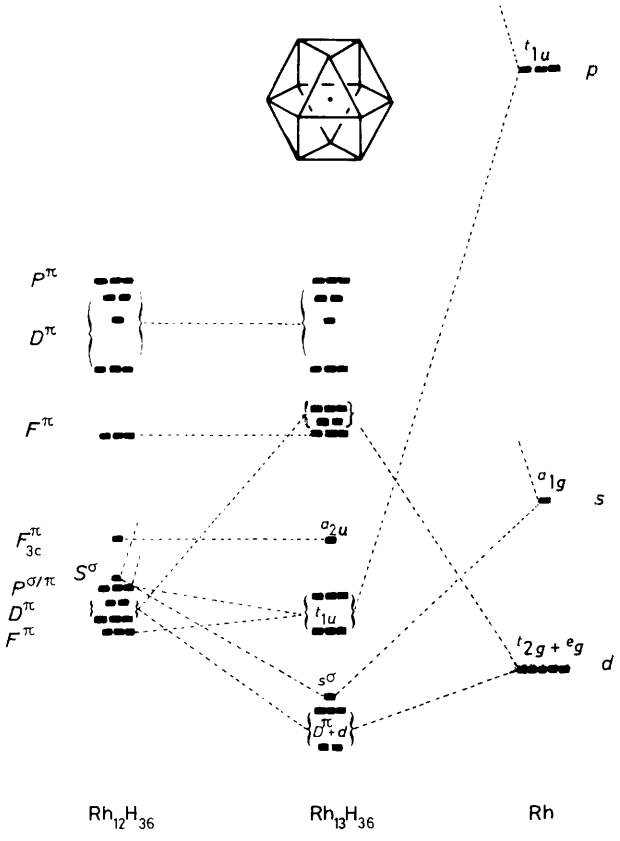

Figure 1. M.o. interaction diagram for a centred cuboctahedron

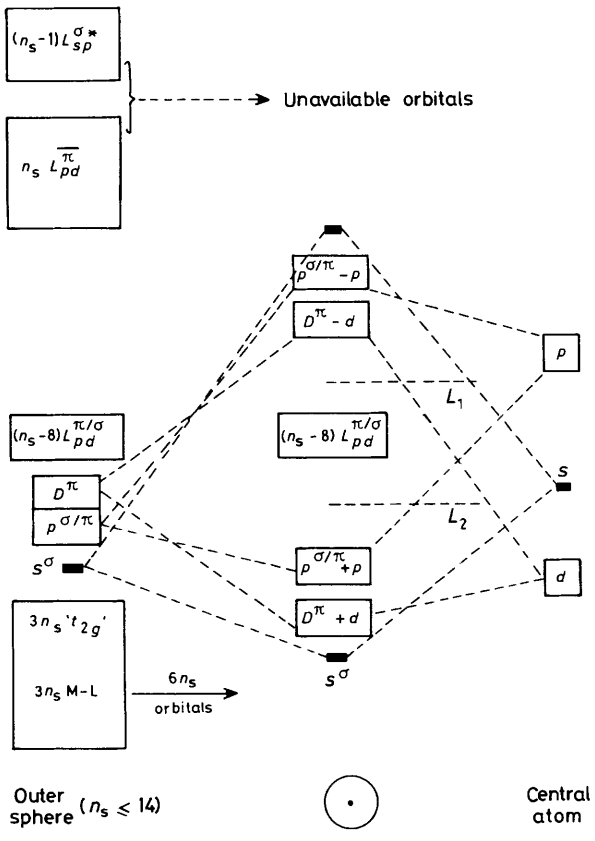

Figure 2. M.o. interaction scheme for a centred spherical cluster

arrangements are small and not predictable from symmetry-based arguments of the type developed in this paper.

From Figure 2 it is apparent that if the orbitals are filled up to level L_1 the total number of available skeletal molecular orbitals is $n_s + 1$ for $n_s \leqslant 14$ and 15 if $n_s > 14$. Some examples of such high-nuclearity clusters are summarized in Table 1. The structures of $[Rh_{13}H_5(CO)_{24}]$ and $[Rh_{12}Pt(CO)_{24}]^{4-}$ are based on h.c.p., $[Os_{10}C(CO)_{24}]^{2-}$ on f.c.c, and $[Rh_{15}(CO)_{30}]^{3-}$ on b.c.c. arrangements.

For the late transition metals and the heavier post-transition metals the *nd* valence orbitals become more core-like and $(n + 1)s$ valence orbitals experience a relativistic contraction and consequently the $(n + 1)p$ valence orbitals are not as accessible for skeletal and metal–ligand bonding. The molecular orbitals (m.o.s) in Figure 2 are filled only to the level L_2 because the $(n_s - 8)L^{\pi/\sigma}_{pd}$ orbitals are much less strongly bonding than the nine S^{σ}, $P^{\sigma/\pi}$, and $D^{\pi/\sigma}$ skeletal m.o.s. Such spherical clusters are characterized by a total of $12n_s + 18$ valence electrons. Examples of such clusters are summarized in Table 2. The metal atoms in $[Au_9(PPh_3)_8]^+$ adopt a cubic arrangement, and those in $[Au_{11}I_3(PPh_3)_7]$ and $[Au_{13}Cl_2(PMe_2Ph)_{10}]^{3+}$ close-packed arrangements based on an icosahedron. In $[Pt_{15}H_x(CO)_8(PBu_3)_6]$ there are 12 atoms cuboctahedrally arranged on the first spherical surface and four capping atoms. This bonding analysis predicts that the number of unlocated hydrido-ligands is eight.

In those clusters described above the metal atoms on the first spherical surface are evently distributed and therefore have a spherical topology. For reasons that have been discussed in some detail elsewhere [5c] if these atoms have a toroidal topology then one of the $P^{\sigma/\pi}$ skeletal m.o.s is no longer bonding and such clusters are characterized by a total of $12n_s + 16$ valence electrons, *e.g.* $[Au_9(PPh_3)_8]^{3+}$.

The compounds described above represent clear-cut situations where the $(n_s - 8)L^{\pi/\sigma}_{pd}$ orbitals are either all utilized or not utilized at all. In Table 3 some examples of clusters which represent intermediate situations are given. In $[Pd_{23}(CO)_{22}(PEt_3)_{10}]$ the central atom is surrounded by 18 metal atoms which are part of a face-centred cubic (f.c.c.) lattice. Six of the metal atoms are at the vertices of an octahedron, 12 additional metal atoms are located at the midpoints of the edges of this octahedron, and the remaining four metal atoms cap the faces of octahedron. The total number of valence electrons is 294, *i.e.* $12n_s + 30$, corresponding to the occupation of the six $L^{\pi/\sigma}_{pd}$ $(L > 2)$ skeletal molecular orbitals for close-packed arrangements as noted above.

In $[Pd_{23}(CO)_{20}(PEt_3)_8]$ and $[Pt_{24}(CO)_{30}]^{2-}$ only two and three $L^{\pi/\sigma}_{pd}$ orbitals are occupied and therefore they represent an intermediate situation in Figure 2, where electron occupation between the L_1 and L_2 levels is occurring. The occurrence of these exceptions is not too surprising in view of the way in which the *d–p* promotion energies of Pd and Pt lead to 18- and 16-electron mononuclear complexes.

(2) *The Bonding in High-nuclearity Clusters with a Deltahedral Interstitial Moiety.*—The molecular-orbital calculation on $Rh_{13}H_{36}$ with one interstitial atom indicated that the *d* orbitals of the central atom play an important bonding role by interacting with D^{π} functions of the atoms on the outer sphere. This suggests that the *d* orbitals in the inner bare cluster will also play an important role for the higher-nuclearity clusters. The 't_{2g}' sets of the inner polyhedron in a high-nuclearity transition-metal cluster consist of L^{σ}_d, L^{δ}_d, and $\overline{L^{\delta}_d}$. As an isolated cluster, these orbitals are effectively metal–metal non-bonding. However, as an interstitial moiety they can accept electrons

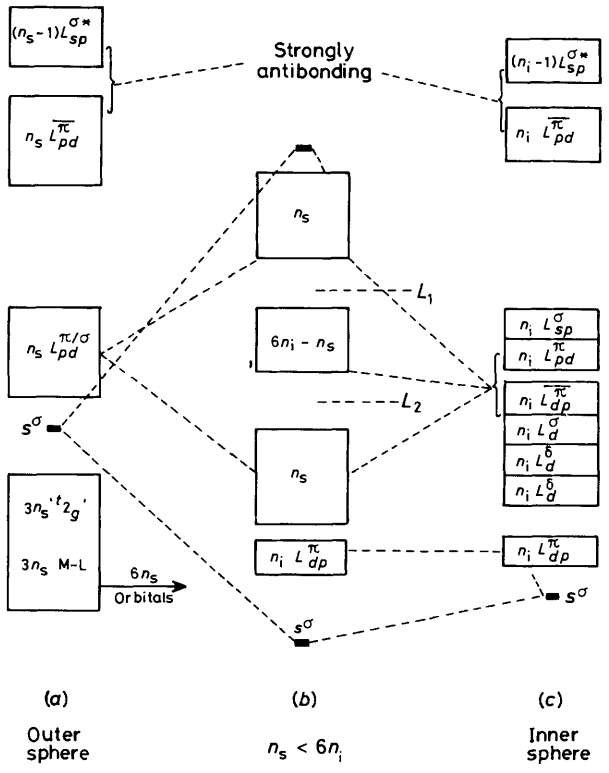

Figure 3. M.o. interaction scheme for a high-nuclearity cluster based on two concentric spheres when $n_s < 6n_i$

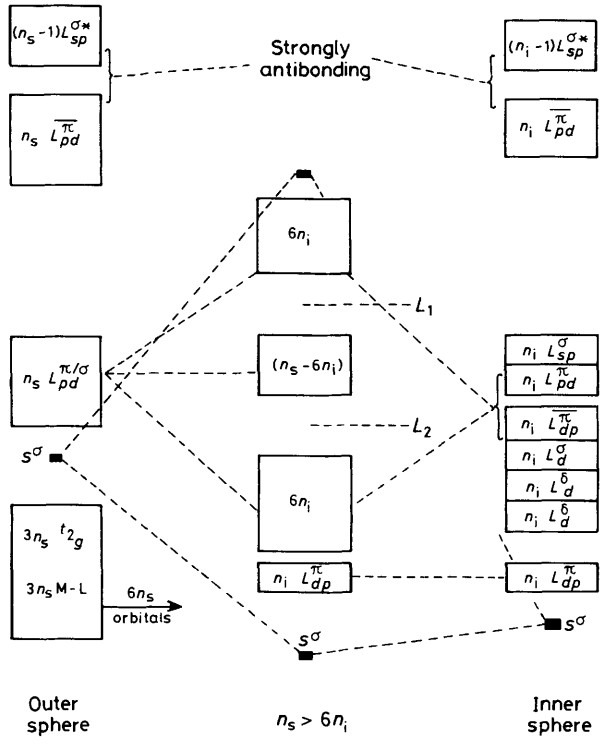

Figure 4. M.o. interaction scheme for a high-nuclearity cluster based on two concentric spheres when $n_s > 6n_i$

from the outer-sphere metal atoms. The latter therefore behave like ligands towards the inner-sphere polyhedron.

Figure 3 gives a schematic fragment-orbital interaction diagram for the outer-sphere and inner-sphere interactions in such a high-nuclearity cluster; n_s indicates the number of atoms on the surface of the outer sphere, n_i the number of atoms on the surface of the inner sphere. Figure 3(*c*) shows the molecular-orbital level diagram of the inner bare cluster which has a deltahedral geometry. From Stone's tensor surface harmonic analysis[6] it has been shown that there are $2n_i - 1$ unavailable orbitals and $7n_i + 1$ available orbitals in deltahedral clusters.[5b] Of the $7n_i + 1$ available orbitals,[5b,6b] the $n_iL_{dp}^{\pi}$ orbitals are inwardly hybridized bonding orbitals, *i.e.* the skeletal bonding orbitals; $n_iL_{pd}^{\pi}$, $n_iL_{sp}^{\sigma}$, and $n_i\overline{L_{dp}^{\pi}}$ (total $3n_i$) are out-pointing orbitals which are the acceptor orbitals for ligand electron pairs and lead to M–L bonding molecular orbitals in low-nuclearity clusters. The $n_iL_d^{\sigma}$, $n_iL_d^{\delta}$, and $n_i\overline{L_d^{\delta}}$ ($3n_i$) orbitals reprsent the 't_{2g}' set. When interactions with the outer sphere are introduced, the $6n_i$ orbitals, $3n_i$ out-pointing and $3n_i$ 't_{2g}' set of orbitals, are very important for interacting with the symmetry-adapted orbitals of the outer sphere. The $n_iL_{dp}^{\pi}$ skeletal bonding orbitals will be less important because they are inwardly hybridized.

Figure 3(*a*) illustrates the orbital pattern of the outer-sphere cluster with ML_3 fragments. The $3n_s$ M–L and $3n_s$ 't_{2g}' sets are out-pointing orbitals in a similar fashion to those discussed above and are less important for interacting with the inner-sphere metal atoms. Occupation of these $6n_s$ orbitals leads to a contribution of $12n_s$ electrons to the total number of valence electrons. The primary bonding interactions with the inner-sphere polyhedron occur through the n_s $L_{pd}^{\pi/\sigma}$ and S^{σ} skeletal bonding orbitals shown in Figure 3(*a*).

When the inner and outer spheres are allowed to interact together to form a bi-spherical cluster, the results depend on whether $n_s > 6n_i$ or $n_s < 6n_i$. If $n_s > 6n_i$ then there are a sufficient number of metal atoms in the outer sphere formally to donate electrons into the $3n_i$ out-pointing and $3n_i$ 't_{2g}'-like orbitals of the inner polyhedron. Figure 3(*b*) illustrates the results of the interaction between inner and outer spheres when $n_s < 6n_i$. The figure indicates that the S^{σ} orbital of the outer sphere interacts strongly with S^{σ} of the inner sphere and gives rise to one antibonding and one strongly bonding orbital; the $n_sL_{pd}^{\pi/\sigma}$ orbitals of the outer sphere interact strongly with n_s orbitals from the $6n_i$ group with the same symmetry and give rise to n_s bonding and n_s antibonding orbitals. The $(6n_i - n_s)$ orbitals from the inner sphere remain essentially non-bonding. If the inner sphere is not covered completely by the atoms in the outer sphere, the $(6n_i - n_s)$ orbitals may be stabilized by interactions with bridging carbonyl ligands and are stabilized sufficiently to be occupied. Consequently, if the molecular orbitals are filled up to the L_1 line in Figure 3, the total number of valence electrons required is $2(6n_s + 7n_i + 1) = 12n_s + 14n_i + 2$, where $14n_i + 2$ corresponds to the characteristic number of electrons for the interstitial deltahedral moiety. If the interstitial group is not deltahedral, the $14n_i + 2$ component is replaced by an alternative number which reflects the structure of the interstitial moiety. This analysis therefore provides a theoretical justification for Mingos' $12n_s + \Delta_i$ electron-counting rule for high-nuclearity clusters. Examples of clusters following this electron-counting rule are listed in Table 2. If the $(6n_i - n_s)$ orbitals are not completely filled, the electron count will be less than $12n_s + \Delta_i$, for example $[Pd_{38}(CO)_{28}(PEt_3)_{12}]$[18] in Table 3, where the interstitial moiety is a tetrahedron, has $12n_s + 52$ valence electrons rather than $12n_s + 60$.

Figure 4 shows the interactions between the outer-sphere atoms and the inner-sphere deltahedron when $n_s > 6n_i$. This differs from Figure 3 because there are now $6n_i$ rather than n_s molecular orbitals stabilized by the inner- and outer-sphere interactions. When the molecular orbitals are filled up to the L_1 line, the electron count is $2[6n_s + (n_i + n_s + 1)]$. When the

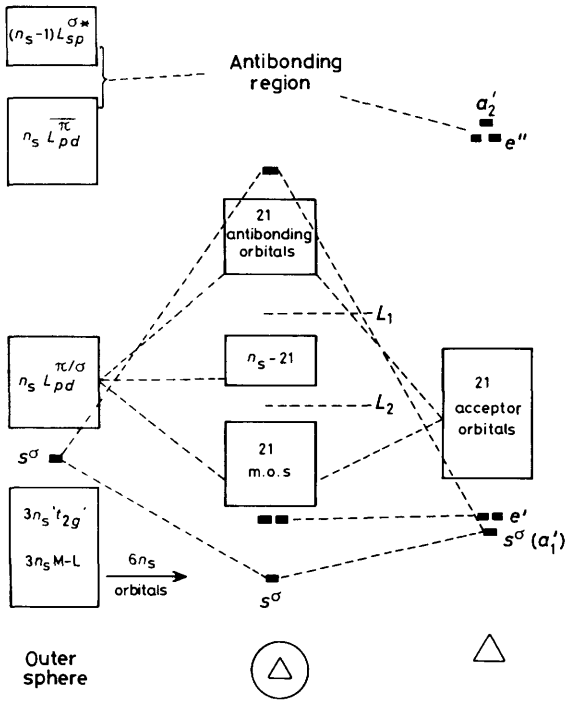

Figure 5. M.o. interaction scheme for a high-nuclearity cluster with a triangular interstitial moiety

electrons are filled up to the L_2 line, the electron count is again the $12n_s + \Delta_i$ derived above in Figure 3. The situation illustrated in Figure 4 is not commonly observed in cluster compounds because for pure geometric reasons the condition $n_s > 6n_i$ is not satisfied for those atoms lying on the second sphere in a close-packed structure.

(3) *The Bonding in High-nuclearity Clusters with Two or Three Interstitial Atoms.*—When the interstitial moiety in a high-nuclearity cluster is a triangular fragment, there are 21 acceptor orbitals for interacting with the outer sphere rather than 18 ($6n_i$), because there are 12 out-pointing orbitals. Each metal atom has four orbitals capable of accepting electrons from ligands. In the isolated cluster this leads to a triangular cluster based on ML_4 fragments. In addition each metal atom has a 't_{2g}' set, leading to nine non-bonding orbitals. Occupation of these 21 acceptor orbitals and the a_1' and e' skeletal bonding molecular orbitals leads to the 48-electron count commonly associated with triangular clusters, such as $[Os_3(CO)_{12}]$. The interaction diagram for a triangular bare cluster with a large polyhedron is illustrated in Figure 5. The molecular orbitals of the inner triangle shown on the right-hand side of the Figure include the $a_1' + e'$ metal–metal bonding orbitals, 21 acceptor orbitals, and $a_2' + e''$ metal–metal antibonding orbitals (27 in total). Interaction with the metal atoms on the outer sphere leads to the stabilization of 24 orbitals through the S^σ and $n_s L_{pd}^{\pi/\sigma}$ in-pointing orbitals. In addition there are $(n_s - 21)$ approximately non-bonding orbitals derived from this set. The occupation of orbitals up to the L_2 line in Figure 5 leads to an electron count of $12n_s + 48$, *i.e.* they also conform to the pattern $12n_s + \Delta_i$. In $[Pt_{26}(CO)_{32}]^{2-}$ [2] the total number of valence electrons is 326, *i.e.* $12n_s + 50$, and Δ_i is 50 rather than 48 for a triangular interstitial moiety. A detailed analysis of the bonding in raft clusters has shown that the addition of edge-bridging metal atoms to a triangular cluster leads to a stabilization of the a_2' ($\overline{P_0^\pi}$) antibonding skeletal molecular orbital. This orbital is sufficiently stabilized in a planar six-atom cluster to be occupied by an additional electron pair.[19] Therefore, we propose that in high-nuclearity clusters with an interstitial triangular moiety the a_2' orbital is utilized in bonding leading to a characteristic electron count of $12n_s + 50$ rather than $12n_s + 48$ if there are more than three surface atoms coplanar with the triangle.

When the geometry of the three interstitial atoms is linear, the bonding scheme is slightly different from Figure 5. The $a_1' + e'$ three metal–metal bonding orbitals on the right-hand side of Figure 5 are replaced by two metal–metal bonding orbitals (one is S^σ, the other is P_z^σ if the z axis is defined along the M–M–M bonding direction); there are now 23 acceptor orbitals because the terminal metal atoms each have an additional out-pointing orbital. Interaction with the metal atoms on the outer sphere leads to a stabilization of 25 orbitals. In addition there are $(n_s - 23)$ approximately non-bonding orbitals derived from the outer sphere. Consequently, the occupation of orbitals up to the L_2 line leads to an electron count of $12n_s + 50$, *i.e.* $12n_s + \Delta_i$. The compound $[Au_{13}Ag_{12}Cl_6(PPh_3)_{12}]^{m+}$ provides an example of such a cluster (see Table 2), but unfortunately it has not been sufficiently characterized to provide unambiguous support for the predicted electron count. If the orbitals are filled up to the L_1 line, the electron count is $12n_s + 2(n_s + 2)$.

When the interstitial moiety in a high-nuclearity cluster is a diatomic fragment, there are 16 acceptor orbitals for interacting with the outer sphere rather than 12 ($6n_i$), because there are 10 out-pointing orbitals in which each metal atom has five orbitals capable of accepting electrons from ligands. In the isolated cluster, this leads to a diatomic cluster based on two ML_5 fragments, such as $[Mn_2(CO)_{10}]$. In addition each metal atom has a 't_{2g}' set, leading to six non-bonding orbitals. Occupation of these 16 orbitals and the S^σ metal–metal bonding orbital leads to the 34-electron count. The interaction scheme between the interstitial diatomic fragment and outer sphere is different from Figure 5. Now there is only one S^σ metal–metal bond orbital rather than three for the triangular moiety. The interaction between S^σ from the interstitial moiety and S^σ from the outer sphere leads to one bonding and one antibonding orbital. The 16 acceptor orbitals interact with 16 symmetry-adapted orbitals from $n_s L_{pd}^{\pi/\sigma}$ set of the outer sphere. Consequently, the number of skeletal molecular orbitals below the L_2 level (compared with Figure 5) is 17. In addition, there are $(n_s - 16)$ skeletal molecular orbitals present between the L_1 and L_2 levels. Therefore, occupation of orbitals up to the L_2 level leads to 17 skeletal bonding orbitals, corresponding to $12n_s + 34$, *i.e.* $12n_s + \Delta_i$. There are two examples of clusters following this electron count, $[Pt_{19}(CO)_{22}]^{4-}$ and $[Rh_{22}H_{5-q-m}(CO)_{35}]^{q-}$, listed in Table 2. If the orbitals are filled up to the L_1 level, the number of skeletal bonding orbitals is $n_s + 1$, corresponding to the $12n_s + 2(n_s + 1)$ electron-counting rule which is the same as the case where there is only one interstitial atom. In $[Rh_{22}H_{5-q-m}(CO)_{35}]^{q-}$ the two interstitial atoms are surrounded by 16 metal atoms lying on the first spherical surface. The remaining four metal atoms cap the square faces of the polyhedron. Therefore, for $[Rh_{22}H_{5-q-m}(CO)_{35}]^{q-}$ there are no $L_{pd}^{\pi/\sigma}$ orbitals between the L_1 and L_2 levels and its $n_s + 1$ (17) skeletal bonding orbitals are consistent with both the $12n_s + 2(n_s + 1)$ rule and the $12n_s + \Delta_i$ rule.

Summary of conclusions for high-nuclearity transition-metal clusters. The analyses developed above have indicated two limiting types of bonding in high-nuclearity clusters. The majority of such clusters have electron counts which can be summarized by the $12n_s + \Delta_i$ rule. In terms of the Stone spherical harmonic notation this corresponds to the occupation of a set of molecular orbitals which can be correlated with the skeletal (s_1) and acceptor (a_1) orbitals of the interstitial cluster [$\Delta_i = 2(s_i + a_i)$] and $6n_s$ metal–ligand and non-bonding orbitals of the outer-sphere metal atoms. Previously this mode of bonding has been described as radial in order to emphasize

the donation of electrons from orbitals of the outer-sphere atoms to the available orbitals of the interstitial cluster.

The molecular-orbital schemes in Figures 2 and 4 also suggest alternative electron counts corresponding to filling up to the L_1 level. The additional number of orbitals lying between the L_2 and L_1 levels depends on the number of metals contained in the interstitial moiety and their geometry. In general there are $(n_s - a_i)L_{pd}^{\pi/\sigma}$ molecular orbitals which are localized predominantly on the outer-sphere atoms and are tangential in nature. These additional tangential molecular orbitals are only significant for those clusters of metals with low *d–p* promotion energies and low nuclearities. The number of orbitals lying between L_1 and L_2 begins to approach zero as the nuclearity increases. The quantum number L of the relevant orbitals also increases and the corresponding $L_{pd}^{\pi/\sigma}$ orbitals become less strongly bonding.

For this second category of cluster the electron count can also be expressed as $12n_s + 2(s_i + a_i) + 2(n_s - a_i) = 12n_s + 2(s_i + n_s)$. The outer sphere contains a large number of atoms distributed evenly on the surface of the sphere and is characterized by a total of $n_s + 1$, *i.e.* s_s, skeletal bonding molecular orbitals. Therefore, these clusters where tangential bonding on the surface is significant are associated with a total number of valence electrons $12n_s + 2(s_i + s_s - 1)$. The results of these alternative bonding modes are summarized in Table 4. The occurrence of significant tangential bonding is particularly important for smaller clusters with main-group interstitial moieties.

(4) *The Bonding in High-nuclearity Clusters with More Complex Interstitial Moieties.*—The interstitial moiety in high-nuclearity clusters is not limited to transition metals. There are clusters with interstitial main-group atoms linked together and combinations of main-group and transition metals. When the interstitial moiety is a group of main-group atoms, then the situation is similar to Figure 4 because the number of orbitals contributed by the surface atoms greatly exceeds the number of acceptor orbitals associated with the interestitial moiety. For main-group fragments there are only n_i acceptor orbitals rather than $6n_i$ if the interstitial moiety is either deltahedral or three-connected since each vertex has one out-pointing orbital capable of accepting one pair of electrons from a ligand (for example, in *closo*-borane clusters each B atom forms a single bond with an H atom). Therefore, the bonding scheme is similar to that shown in Figure 4 but the $6n_i$ acceptor orbitals are replaced by n_i acceptor orbitals. Consequently, there are $(2n_i + 1)$ (*i.e.* Δ_i) orbitals below the L_2 line and $(n_s - n_i)$ orbitals between the L_1 and L_2 lines.

The resulting electron counts for a cuboctahedral interstitial moiety are either $12n_s + \Delta_i$ or $12n_s + 2(n_s + n_i + 1)$. For a cuboctahedral or icosahedral fragment inside a truncated octahedron of nickel atoms, this would correspond to electron counts of 434 $(12n_s + \Delta_i)$ or 474 $[12n_s + 2(n_s + n_i + 1)]$ and could be realized in the clusters $[Ni_{32}B_{12}(CO)_{39}]$ and $[Ni_{32}B_{12}(CO)_{59}]$. The latter results in the occupation of surface tangential molecular orbitals on the metal sphere in addition to the tangential borane L_p^{π} orbitals, but requires an unsatisfactory large number of carbonyl ligands, therefore, for large interstitial main-group fragments the $12n_s + \Delta_i$ electron-counting rule is likely to be more relevant. However, for small interstitial main-group fragments, *e.g.* C_2, the $12n_s + 2(s_i + s_s - 1)$ rule is likely to predominate. In the dicarbidotransition-metal clusters, the s_i for the interstitial C_2 fragment is formally equal to 1. The electron count $12n_s + 2(s_i + s_s - 1) = 12n_s + 2s_s$ is the same as the situation discussed above for high-nuclearity clusters with only one interstitial atom. Therefore the electron count is independent of the interactions between the two interstitial carbon atoms. For example, in the cluster $[Ni_{16}C_4(CO)_{23}]^{4-}$,[20] the interstitial moiety is the four carbon atoms consisting of two C_2 fragments with a separation of 2.88 Å. The total number of valence electrons is $226 = 12 \times 16 + 2(16 + 1)$ with the $n_s + 1$ skeletal electron pairs, corresponding to the occupation of skeletal molecular orbitals up to the L_1 line for the high-nuclearity clusters with two interstitial atoms discussed in section (3). A more detailed theoretical analysis has indicated[17] that the C–C separation in the dicarbido-clusters depends critically on the geometric constraints imposed by the metal cage, and the number of skeletal bonding orbitals is independent of the distance between the two carbon atoms.

Table 4. Summary of electron-count rules

Interstitial moieties		Rule 1 (Radial bonding)	Rule 2 (Radial + tangential bonding)
One interstitial atom		$12n_s + 18$	$12n_s + 2(n_s + 1)$
Two interstitial atoms		$12n_s + 34$	$12n_s + 2(n_s + 1)$
Three interstitial atoms	Triangle	$12n_s + 48$ (or 50)	$12n_s + 2(n_s + 3)$*
	Linear M–M–M	$12n_s + 50$	$12n_s + 2(n_s + 2)$*
	Linear M=M=M	$12n_s + 46$*	$12n_s + 2(n_s + 4)$
	Linear X=M=X	$12n_s + 26$*	
Deltahedral moiety		$12n_s + 14n_i + 2$	$12n_s + 2(n_s + n_i + 1)$*
General cases		$12n_s + \Delta_i$	$12n_s + 2(s_s + s_i - 1)$

* No example of those electron counts.

When the interstitial moiety contains both main-group and transition metals it is necessary to calculate the number of available orbitals (the total of s_i and a_i) associated with the total fragment. In general this can be derived from that calculated for the interstitial transition-metal fragment and subtracting five orbitals for each main-group atom. For example, in $[Ni_{38}C_6(H)(CO)_{42}]^{5-}$,[21] the interstitial moiety is a cube of nickel atoms capped on each face by μ_4-carbido-ligands. A hexacapped-cubic transition-metal cluster is associated with 12 skeletal bonding molecular orbitals[8] and 192 valence electrons, *i.e.* it has 96 valence orbitals available. The related Ni_8C_6 fragment has 66 available orbitals. Therefore the corresponding cluster is calculated to have $12n_s + 132$ valence electrons, *i.e.* 492, very close to the observed electron count of 494. The additional electron pair probably resides in a second S^{σ} orbital which is out of phase between carbon and the interstitial atoms.

In $[Ni_{34}C_4(H)(CO)_{38}]^{5-}$ and $[Ni_{35}C_4(CO)_{39}]^{6-}$[22] the interstitial moiety is a rhombus of nickel atoms with four edge-bridging μ-carbido-ligands. A rhombic transition-metal cluster has 62 valence electrons, *e.g.* $[Re_4(CO)_{16}]^{2-}$, and a tetra-edge-bridged rhombus, $62 + 14 \times 4 = 118$ valence electrons, *i.e.* 59 available orbitals.[19] The corresponding Ni_4C_4 moiety has 39 available orbitals. The following electron counts are therefore calculated, 438 for $[Ni_{34}C_4(H)(CO)_{38}]^{5-}$ and 450 for $[Ni_{35}C_4(CO)_{39}]^{6-}$, in complete agreement with the observed electron counts (see Table 2). In these high-nuclearity nickel clusters the radial bonding model is again dominant and the $12n_s + \Delta_i$ rule is applicable. However, for lower-nuclearity clusters the occupation of tangential orbitals on the outer sphere can also occur. For example the $[Rh_{17}S_2(CO)_{32}]^{3-}$[23] cluster has a four-connected Rh_{16} outer-sphere polyhedron and an interstitial SRhS moiety. The Rh–S bond length in the interstitial moiety is 2.168 Å which is substantially shorter than the Rh–S single-bond length of 2.34 Å, suggesting substantial multiple Rh–S bonding in the former. The total number of valence electrons in the cluster is 232, $12n_s + 40$, corresponding

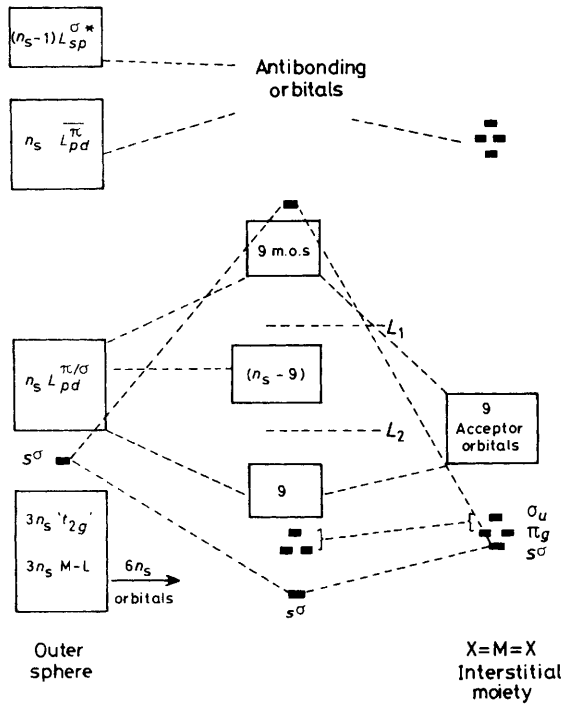

Figure 6. M.o. interaction scheme for a high-nuclearity cluster with a X=M=X interstitial moiety

to 20 skeletal electron pairs. The relevant orbital-interaction diagram for $[Rh_{17}S_2(CO)_{32}]^{3-}$ is shown in Figure 6. The orbitals on the right-hand side associated with the S=Rh=S moiety consist of S^σ and P^σ Rh–S σ-bonding orbitals and two S–Rh–S π-bonding orbitals, which are matched by a set of four antibonding molecular orbitals. There remain a set of nine acceptor orbitals associated with the SRhS fragment. The molecular orbitals characteristic of a four-connected cluster are shown on the left-hand side of the figure. The interaction between these two sets of orbitals leads to nine stable molecular orbitals localized predominantly on the interstitial moiety (radial) and $(n_s - 9)$ $L_{pd}^{\pi/\sigma}$ tangential orbitals localized predominantly on the outer sphere. Occupation of the tangential and radial molecular orbitals leads to a total of $n_s + 4$ skeletal bonding molecular orbitals. For $[Rh_{17}S_2(CO)_{32}]^{3-}$ with $n_s = 16$ this leads to a total of 20 skeletal bonding molecular orbitals and an electron count in complete agreement with the observed electron count.

Conclusions

This paper has demonstrated that it is possible to apply the spherical harmonic methodology to high-nuclearity transition-metal carbonyl cluster compounds. It is remarkable how the closed-shell requirements of these extremely complex chemical entities can be rationalized in terms of a simple model based on the development of a particle-on-a-sphere problem. The high-nuclearity clusters provide a reasonable approximation for this analysis because the metal atoms lie on concentric spheres and the pseudo-spherical symmetry labels can be used to identify the important interactions between atoms on successive layers. The majority of high-nuclearity clusters conform to two electron-counting rules which are summarized in Table 4. If radial and tangential bonding interactions are important for the metal atoms lying on the outer sphere and there is more than one interstitial atom, the relevant electron-counting rule can be expressed as $12n_s + 2(s_s + s_i - 1)$ where s_s and s_i are the number of skeletal bonding molecular orbitals associated with the surface (s_s) and interstitial (s_i) moieties. This rule is particularly relevant to clusters of rhodium with 12—20 surface atoms and main-group interstitial fragments.

For the late transition metals and clusters containing several interstitial metal atoms the radial interactions in the cluster are particularly important and the surface atoms donate electron density to the acceptor orbitals of the interstitial moiety. These clusters are characterized by the electron-counting rule $12n_s + \Delta_i$ where Δ_i is the electron count associated with the interstitial moiety. Some examples of such clusters are given in Table 2. The interstitial moiety has a set of skeletal bonding molecular orbitals which are similar to those for the isolated cluster. In addition the $6n_i$ orbitals which are either non-bonding or metal–ligand bonding are involved in metal–metal bonding interactions with the surface metal atoms.

Appendix

The calculations were performed within the extended-Hückel method.[24] The exponents of the rhodium atom were taken from the literature.[25] For the rhodium atoms $H_{ii}(s) = -9.59$ eV and $H_{ii}(p) = -4.57$ eV. For the surface rhodium atoms $H_{ii}(d) = -12.5$ eV and $H_{ii}(d) = -11.0$ eV for the central rhodium atom. This distinction compensated for the approximation of using hydrogen atoms to replace the carbonyl ligands in the real molecules and led to satisfactory highest occupied molecular orbital (h.o.m.o.) – l.u.m.o. energy gaps. The following bond lengths were used in the calculations: Rh–Rh 2.75 and Rh–H 1.80 Å.

Acknowledgements

The S.E.R.C. and the Chinese Academy of Sciences are thanked for their financial support and Dr. R. L. Johnston for helpful comments.

References

1 P. Chini, G. Longoni, and V. G. Albano, *Adv. Organomet. Chem.*, 1976, **14**, 285.
2 P. Chini, *J. Organomet. Chem.*, 1980, **200**, 37.
3 M. D. Vargas and J. N. Nicholls, *Adv. Inorg. Chem. Radiochem.*, 1986, **30**, 123.
4 A. Ceriotti, F. Demartin, G. Longoni, M. Manassero, M. Marchionna, G. Piva, and M. Sansoni, *Angew. Chem., Int. Ed. Engl.*, 1985, **24**, 697.
5 (*a*) D. M. P. Mingos, *J. Chem. Soc., Chem. Commun.*, 1985, 1353; (*b*) *Chem. Soc. Rev.*, 1986, **15**, 31; (*c*) K. P. Hall, D. I. Gilmour, and D. M. P. Mingos, *J. Organomet. Chem.*, 1984, **268**, 275.
6 A. J. Stone, (*a*) *Mol Phys.*, 1980, **41**, 1339; (*b*) *Inorg. Chem.*, 1981, **20**, 256; (*c*) *Polyhedron*, 1984, **3**, 1299.
7 B. K. Teo and N. A. J. Sloane, *Inorg. Chem.*, 1985, **24**, 4545.
8 R. L. Johnston and D. M. P. Mingos, *J. Chem. Soc., Dalton Trans.*, 1987, 647, 1445.
9 D. M. P. Mingos and M. I. Forsyth, *J. Chem. Soc., Dalton Trans.*, 1977, 610.
10 (*a*) K. Wade, *Adv. Inorg. Chem. Radiochem.*, 1976, **18**, 1; (*b*) D. M. P. Mingos, *Nature (London), Phys. Sci.*, 1972, **236**, 99; (*c*) M. Elian, M. M. L. Chen, D. M. P. Mingos, and R. Hoffmann, *Inorg. Chem.*, 1976, **15**, 1148.
11 A. Fumagalli, S. Martinengo, and G. Ciani, *J. Chem. Soc., Chem. Commun.*, 1983, 1381.
12 V. G. Albano, G. Ciani, S. Martinengo, and A. Sironi, *J. Chem. Soc., Dalton Trans.*, 1979, 978.
13 J. L. Vidal and J. M. Troup, *J. Organomet. Chem.*, 1981, **213**, 351.
14 S. Sirugi, M. Bianchi, and E. Benedetti, *Chem. Commun.*, 1969, 596.
15 E. R. Corey, L. F. Dahl, and W. Beck, *J. Am. Chem. Soc.*, 1963, **85**, 1202.

16 D. M. P. Mingos and Lin Zhenyang, *J. Organomet. Chem.*, in the press.
17 J-F. Halet and D. M. P. Mingos, *Organometallics*, 1988, **7**, 51.
18 E. G. Mednikov, N. Y. Eremenko, Y. L. Slovokhotov, and Y. T. Struchkov, *J. Chem. Soc., Chem. Commun.*, 1987, 218.
19 D. G. Evans and D. M. P. Mingos, *Organometallics*, 1983, **2**, 435.
20 A. Ceriotti, G. Longoni, M. Manassero, N. Masciocchi, G. Piro, L. Resconi, and M. Sansoni, *J. Chem. Soc., Chem. Commun.*, 1985, 1402.
21 A. Ceriotti, A. Fait, G. Longoni, G. Piro, L. Resconi, F. Demartin, M. Manassero, N. Masciocchi, and M. Sansoni, *J. Am. Chem. Soc.*, 1986, **108**, 8091.
22 A. Ceriotti, A. Fait, G. Longoni, G. Piro, L. Resconi, F. Demartin, M. Manassero, N. Masciocchi, and M. Sansoni, *J. Am. Chem. Soc.*, 1986, **108**, 5370.
23 J. L. Vidal, R. A. Fiato, L. A. Cosby, and R. L. Pruett, *Inorg. Chem.*, 1978, **17**, 2574.
24 R. Hoffman, *J. Chem. Phys.*, 1963, **39**, 1397; R. Hoffmann and W. N. Lipscomb, *ibid.*, 1962, **36**, 2179, 3189; **37**, 2872.
25 R. H. Summerville and R. Hoffmann, *J. Am. Chem. Soc.*, 1976, **98**, 7240.

Received 31*st July* 1987; *Paper* 7/1410